Rock and Soil Mechanics

Volume 41 | Issue 12 Article 3

4-29-2021

A simplified method for geotechnical analysis of energy pile groups

Kang FEI

Zhi-hui ZHU

Yu-heng SHI

Ying ZHOU

Rock and Soil Mechanics 2020 41(12): 3889−3898 ISSN 1000−7598
https: //doi.org/10.16285/j.rsm.2020.5313 rocksoilmech.researchcommons.org/journal

A simplified method for geotechnical analysis of energy pile groups

FEI Kang, ZHU Zhi-hui, SHI Yu-heng, ZHOU Ying
Institute of Geotechnical Engineering, Yangzhou University, Yangzhou, Jiangsu 225127, China

Abstract: A simplified analytical method is proposed for the geotechnical analysis of energy pile groups under thermo-mechanical loads. The relationship between the shear stress and the relative displacement at the pile-soil interface is modeled by a hyperbolic function. The elastic shear displacement method is used to determine the deformation of the surrounding soil. Assuming the settlements induced by the adjacent piles are elastic, the shaft and base interactions among piles are considered separately. The effects of the nonlinear behavior at the pile-soil interface, the pile head restraint condition, and the location of energy piles in the pile group can be predicted reasonably. The computed interaction factor between two energy piles by the proposed method are better than those from the elastic approach. The reliability of the present method is also validated with the experimental data collected from literatures. Both the computed and the measured results show that if part of the piles are subjected to the temperature change, the foundation tilting and the redistribution of the axial load among the piles will be induced. The present method can capture the main characteristics of energy pile groups efficiently and be used as a useful analysis tool for the engineering design.

Keywords: energy pile groups; thermo-mechanical loading; interaction; differential settlement; load redistribution

1 Introduction

Energy pile technology refers to burying heat exchange tubes in the ground source heat pump system inside the pile body, and the pile body plays the role of load bearing and heat exchange at the same time, so as to reduce the ground area and construction cost needed for burying heat exchange tubes. Energy pile is an economical and emerging technology, which has gradually gained attention in the industry and academic community[1−2]. In order to ensure the safety and reliability of the energy pile, the working characteristics of the energy pile under thermal-mechanical coupled load have been comprehensively studied by previous scholars. Amatya et al.[3], Gui et al.[4] and Lu et al.[5] tested the changing rules of pile axial force, pile side resistance and pile top displacement under different working conditions through field tests. Ng et al.[6] studied the influence of pile top working load level and pile end support conditions on energy pile working characteristics through centrifuge tests. The experimental results from previous researchers all showed that the pile expands when heated, and the upper and lower pile body deform around a certain point (neutral point) respectively. Due to the pile−soil interaction, the side resistance above the neutral point decreases, while the side resistance below the neutral point increases, resulting in additional compression stress in the pile. Laloui et al.[7] and Rotta et al.[8] also obtained similar behaviors through finite element numerical simulation. Fei et al.[9] took the transfer function as hyperbola, considered the temperature deformation of the pile, and used Mansin's rule to reflect the difference in adding and unloading stiffness in the process of rising and cooling, and established a simplified analysis method for the working characteristics of single energy pile. Huang et al.[10] took the transfer function as an exponential function to improve the calculation method of the depth of the neutral point. Although those methods are more simplified, they can reflect the main rules observed in the experiment and can be used to analyze the working characteristics of single energy pile. In practical engineering, however, energy piles often appear in the form of pile groups. Thus, the working characteristics of energy pile groups are different from that of single pile, and the arrangement of energy piles has impact on the working characteristics of pile groups. These issues are worth studying. Due to the complexity of the issue, relevant research results are rarely reported. Peng et al.[11] conducted small-scale model tests on pile group foundation, and the results showed that the energy pile group would show uneven deformation under the condition of partial heating. Ng et al.[12] pointed out that based on centrifugal test that the non-uniform deformation of foundation pile caused by temperature change would change pile top load. Lu et al.[13] believed that the operation of the energy pile had a certain influence on the stress of the raft. Salciarini et al.[14] analyzed the thermal and mechanical properties of an energy pile group foundation by using three-dimensional finite element method. The results showed that the operation of the energy pile would change the axial force of the energy pile and the ordinary pile, and the axial force change was closely related to the position of the energy pile. Based on the results of numerical analysis, Rotta et al.[15] pointed out that pile group effect in energy pile group foundation cannot be ignored. Although the finite element method can reasonably reflect the constitutive relation, load and boundary conditions of the material, it is also very complex and difficult for application in pile group foundations. Therefore, it is

Received: 19 March 2020 Revised: 1 June 2020
This work was supported by the National Natural Science Foundation of China (51778557).
First author: FEI Kang, male, born in 1978, PhD, Professor, research interests: subgrade and foundation engineering. E-mail: kfei@yzu.edu.cn

still necessary to establish a simplified analysis method for the working characteristics of energy pile groups.

With the help of the interaction factor method of conventional pile group settlement analysis, Rotta et al.[16−17] gave the interaction factors between two energy piles with different length−diameter ratios, pile spacing and pile−soil stiffness ratios by using elastic finite element method. On this basis, the pile top displacement of pile group under uniform temperature rise or drop is obtained by using the elastic superposition principle. Because all the piles are energy piles, this method cannot consider the influence of the position of the energy piles. Moreover, the elastic finite element does not reflect the nonlinear mechanical properties of the pile−soil interface, therefore, the interaction between piles may be overestimated. In addition, the method cannot consider the effect of temperature and mechanical load at the same time, hence its application has some limitations.

In this paper, the hyperbolic model is used to simulate the mechanical behavior on the interface of pile and soil, and the shear displacement method is used to reflect the transfer of shear stress in soil layer. Considering the interaction of pile groups, the governing equations of pile and soil system under thermal mechanical coupled action are derived, and the partial differential solution scheme is given. By using the proposed method, the cases in the literature are compared and verified, and the working characteristics of energy pile foundation are analyzed.

2 Simplified analysis method derivation

2.1 Governing equation for single pile

Similar to the traditional transfer function method, the equilibrium condition of the differential element of pile can be obtained:

$$\frac{\partial N}{\partial z}+2\pi r\tau=0 \tag{1}$$

where N is the axial force, compression is positive; τ is the pile side shear stress, upward is positive; r is the radius of the pile; and z is the depth.

Both temperature and mechanical load are considered. If the strain is defined as positive as compression and the temperature as positive as increase, there is

$$\varepsilon=-\frac{\partial u}{\partial z}=\frac{N}{E_{\mathrm{p}}A}-\alpha_{\mathrm{T}}\Delta T \tag{2}$$

where ε, E_{p}, A, α_{T} and ΔT are the strain, elastic modulus, cross-sectional area, linear expansion coefficient and temperature increment, respectively.

If the temperature increment is assumed to remain constant along the pile length, combing Eqs. (1) and (2) yields:

$$-E_{\mathrm{p}}A\frac{\partial^2 u}{\partial z^2}+2\pi r\tau=0 \tag{3}$$

or

$$\tau=\frac{E_{\mathrm{p}}A}{2\pi r}\frac{\partial^2 u}{\partial z^2} \tag{4}$$

Equation (3) is consistent with the governing equation of the traditional load transfer method. The difference lies in the relationship between shear stress and displacement and different boundary conditions, which will be introduced together in the solution of pile group problem.

2.2 Mechanical behavior at the pile−soil interface

2.2.1 Mechanical behavior along the pile side

Studies have shown that under the vertical load[18−19], except the local area around the pile, most of the soil is in an elastic state, and the nonlinear characteristics of the load−displacement curve of a single pile mainly depend on the slippage at the pile−soil contact surface. Therefore, the pile displacement u at a certain depth is decomposed into the relative slip displacement s of the pile−soil contact surface and the displacement w of the soil around the pile, namely

$$u=s+w \tag{5}$$

The relationship between slip displacement s and pile side shear stress τ can be simulated by hyperbola as follows:

$$\tau=\frac{s}{a+bs} \tag{6}$$

where a and b are model parameters, which are determined by the following formula:

$$a=\frac{(1-R_{\mathrm{f}})s_{\mathrm{f}}}{\tau_{\mathrm{f}}} \tag{7}$$

$$b=1/\tau_{\mathrm{u}}=R_{\mathrm{f}}/\tau_{\mathrm{f}} \tag{8}$$

where τ_{u} is the asymptotic value of the hyperbola; τ_{f} is the pile side friction strength; R_{f} is the failure stress ratio, ranging between 0.85 and 0.95; and s_{f} is the slip displacement when the shear stress reaches the failure strength, generally between 2 and 4 mm.

The elastic displacement w in the soil is calculated according to the shear displacement method of Randolph et al.[19]:

$$w=\frac{r}{G}\ln\left(\frac{r_{\mathrm{m}}}{r}\right)\tau \tag{9}$$

where G is the soil shear modulus; r_{m} is the influence radius of pile, in homogeneous soil $r_{\mathrm{m}}=2.5l(1-\nu)$; l is the pile length; and ν is the Poisson's ratio of soil. By combining Eqs. (5), (6) and (9), the incremental form between pile side shear stress and displacement can be obtained as follows:

$$\delta u=\left[\frac{a}{(1-\tau b)^2}+\frac{r}{G}\ln\left(\frac{r_{\mathrm{m}}}{r}\right)\right]\delta\tau \tag{10}$$

The energy pile will expand and shrink repeatedly in the process of heating and cooling, and the soil around the pile will be loaded and unloaded to different degrees.

Literature research[9] considers the difference of loading and unloading moduli through Mansin's law. However, Manxin's law is applicable to regular loading and unloading conditions. For irregular loading, upper skeleton and upper large circle rules are needed to avoid unreasonable situations such as stress−strain curve exceeding the limit stress, and the actual judgment is relatively complicated. In this paper, Pyke method[20] was used to construct loading and unloading stress−strain curves. Unloading and reverse loading curves were obtained according to stress skeleton curves:

$$\frac{\tau-\tau_{\mathrm{c}}}{R}=\frac{\left(\dfrac{s-s_{\mathrm{c}}}{R}\right)}{a+b\left|\dfrac{s-s_{\mathrm{c}}}{R}\right|} \tag{11}$$

where τ_{c} and s_{c} are the stress and displacement when the stress−displacement curve turns. $R=\left|\pm1-\tau_{\mathrm{c}}/\tau_{\mathrm{u}}\right|$, load for plus, unload for minus. The corresponding tangent stiffness can be obtained by differentiating Eq. (11), then Eq. (10) can be rewritten as

$$\delta u=C\delta\tau \tag{12}$$

where $C=\dfrac{aR^2}{\left[R-b\left|\tau-\tau_{\mathrm{c}}\right|\right]^2}+\dfrac{r}{G}\ln\left(\dfrac{r_{\mathrm{m}}}{r}\right)$.

2.2.2 Mechanical behavior of pile tip

The relationship between pile end pressure and displacement is simulated by hyperbola:

$$P=\frac{w_{\mathrm{b}}}{f+gw_{\mathrm{b}}} \tag{13}$$

where P is the total pile end stress; w_{b} is the displacement of pile end; f and g are model parameters, which can be determined by the following formula[19]:

$$f=\frac{1-v_{\mathrm{b}}}{4G_{\mathrm{b}}r} \tag{14}$$

$$g=R_{\mathrm{f}}/P_{\mathrm{bf}} \tag{15}$$

where G_{b} and v_{b} are the shear modulus and Poisson's ratio of soil at the pile end, respectively; and P_{bf} is the total ultimate bearing capacity of pile end.

Considering loading and unloading of pile end, the incremental form of Eq. (13) is

$$\delta w_{\mathrm{b}}=C_{\mathrm{b}}\delta P \tag{16}$$

where $C_{\mathrm{b}}=\dfrac{fR^2}{\left[R-g\left|P-P_{\mathrm{c}}\right|\right]^2}$.

2.3 Pile−pile interaction

In pile group foundation, due to the diffusion and transfer of stress in soil, the interaction between piles increases the vertical displacement. If two piles i and j are considered, the displacement increment δu_{iz} of pile i at the depth z can be decomposed into two parts:

$$\delta u_{iz}=\delta u_{iiz}+\delta u_{ijz} \tag{17}$$

where δu_{iiz} is the displacement caused by the load of the ith pile at its location; δu_{ijz} is the displacement generated by the load of the jth pile at the ith pile.

δu_{iiz} contains the slip displacement of the pile−soil interface and the displacement generated by the elastic deformation of the soil, which is calculated according to Eq.(12). Lee et al.[18] showed that the displacement generated by interaction u_{ijz} can be considered as elastic deformation, which can be calculated according to the shear displacement transfer method.

$$\delta u_{ijz}=\frac{r}{G}\delta\tau_{jz}\ln\left(\frac{r_{\mathrm{m}}}{s_{ij}}\right) \tag{18}$$

where s_{ij} is the center distance between piles i and j. When s_{ij} exceeds r_{m}, pile interactions are not considered.

Therefore, in a pile group foundation with n piles, the settlement of any pile i can be expressed as

$$\delta u_{iz}=\sum_{j=1}^{n}C_{ij}\delta\tau_j \tag{19}$$

when $i=j$, $C_{ii}=\dfrac{aR^2}{\left[R-b\left|\tau_{iz}-\tau_{\mathrm{c}}\right|\right]^2}+\dfrac{r}{G}\ln\left(\dfrac{r_{\mathrm{m}}}{r}\right)$; when $i\neq j$, $C_{ij}=\dfrac{r}{G}\ln\left(\dfrac{r_{\mathrm{m}}}{s_{ij}}\right)$.

When conducting pile group analysis under mechanical load, Lee et al.[18] reported that the shear stress of each pile side at the same depth has little difference and can be approximated to the same value. However, for the energy pile foundation, the temperature variation of each pile may be different, and the shear stress will be obviously different, which cannot be combined.

Assuming that the soil displacement increment at the pile tip caused by pile−pile interaction is elastic[21], the increment of pile tip load of the jth pile δP_j causes the increment of pile tip displacement of the ith pile is expressed as

$$\delta w_{\mathrm{b}ij}=\frac{\left(1-v_{\mathrm{b}}\right)}{2\pi G_{\mathrm{b}}s_{ij}}\delta P_j \tag{20}$$

Consequently, in a pile group foundation with n piles, the pile tip settlement of any pile i can be expressed as

$$\delta w_{\mathrm{b}i}=\sum_{j=1}^{n}C_{\mathrm{b}ij}\delta P_j \tag{21}$$

when $i=j$, $C_{\mathrm{b}ii}=\dfrac{fR^2}{\left[R-g\left|P_i-P_{\mathrm{c}}\right|\right]^2}$; when $i\neq j$, $C_{\mathrm{b}ij}=\dfrac{\left(1-v_{\mathrm{b}}\right)}{2\pi G_{\mathrm{b}}s_{ij}}$.

By combining Eqs. (4), (19) and (21), and considering boundary conditions, displacement and internal force of pile group can be solved.

3 Simplified analysis method

In practical engineering, the energy pile should bear the superstructure load first. After the building is put into use, it will play the role of heat transfer according to the requirements of heating or cooling. Therefore, in the simplified analysis method, the response under mechanical load is first calculated, and then the influence of temperature load is considered.

3.1 Governing equations and solutions under mechanical load

Divide n piles into N sections, each section length $\Delta h = L/N$ and a total of M nodes ($M = N+1$). For the l-th node of the i-th pile, using the second-order precision discrete form of the second-order derivative, combined with Eq. (4), Eq. (19) is transformed into

$$\delta u_{i,l} = \sum_{j=1}^{n} C_{ij,l} \frac{E_{\mathrm{p}} A}{2\pi r \Delta h^2} \left(\delta u_{j,l+1} - 2\delta u_{j,l} + \delta u_{j,l-1} \right) \tag{22}$$

Let α represent $\dfrac{E_{\mathrm{p}} A}{2\pi r \Delta h^2}$, Eq. (22) is changed to

$$-\sum_{j=1}^{n} C_{ij,l} \alpha \delta u_{j,l-1} + \left(2\alpha C_{ii,l} + 1\right) \delta u_{i,l} + \sum_{j=1, i \neq j}^{n} 2\alpha C_{ij,l} \delta u_{j,l} - \sum_{j=1}^{n} C_{ij,l} \alpha \delta u_{j,l+1} = 0 \tag{23}$$

For pile top node 1 and pile end node M, in order to ensure the second-order discrete precision, two virtual nodes 0 and M+1 need to be added. The displacement of these two nodes needs to be solved in combination with boundary conditions.

If it is assumed that pile top is connected by raft or bearing platform, under the action of vertical load increment δP, the displacement increment of each pile is equal, i.e.

$$\delta u_{1,1} = \delta u_{2,1} = \cdots = \delta u_{n,1} \tag{24}$$

In addition, the sum of the incremental axial forces on the top of each pile is equal to the external load:

$$\delta N_{1,1} + \delta N_{1,1} + \cdots + \delta N_{n,1} = \delta P \tag{25}$$

Because $\delta N = E_{\mathrm{p}} A \left(\dfrac{\partial \delta u}{\partial z} + \alpha_{\mathrm{T}} \delta T \right)$, under the mechanical load, the influence of temperature is not taken into account, and after discretization with second-order precision difference, it is substituted into Eq. (25), there is

$$\sum_{j=1}^{n} \beta \left(\delta u_{j,0} - \delta u_{j,2} \right) = \delta P \tag{26}$$

where $\beta = E_{\mathrm{p}} A / 2\Delta h$.

For the node of the pile end, $\delta u_{i,M} = \delta w_{\mathrm{b}i}$, the displacement and reaction force of the pile should meet the Eq. (21), after the rearrangement:

$$\sum_{j=1}^{n} C_{\mathrm{b}ij} \beta \delta u_{j,M-1} - \delta u_{i,M} - \sum_{j=1}^{n} C_{\mathrm{b}ij} \beta \delta u_{j,M+1} = 0 \tag{27}$$

Equations (23), (24), (26) and (27) can be written in matrix form:

$$[K]\{\delta u\} = \{\delta F\} \tag{28}$$

where $\{u\}$ is the displacement column vector of all nodes of pile group, and the total number of elements are $L = n \times (M + 2)$.

$$\left.\begin{aligned} \{\delta u\}^{\mathrm{T}} &= \left\{ \{\delta u_1\}^{\mathrm{T}}, \{\delta u_2\}^{\mathrm{T}}, \ldots, \{\delta u_n\}^{\mathrm{T}} \right\} \\ \{\delta u_i\}^{\mathrm{T}} &= \left\{ \delta u_{i,0}, \delta u_{i,1} \cdots, \delta u_{i,M+1} \right\}^{\mathrm{T}} \end{aligned}\right\} \tag{29}$$

where $\{\delta F\}^{\mathrm{T}}$ is the generalized load vector of pile group, when under mechanical loads, only $\delta F_{n,1} = \delta P$ valid in $\{\delta F_n\}^{\mathrm{T}}$, the rest of the elements are all 0.

$$[K] = \begin{bmatrix} [K_{1,1}] & [K_{1,2}] & \cdots & [K_{1,n}] \\ [K_{2,1}] & [K_{2,2}] & \cdots & [K_{2,n}] \\ \vdots & \vdots & \ddots & \vdots \\ [K_{n,1}] & [K_{n,2}] & \cdots & [K_{n,n}] \end{bmatrix} \tag{30}$$

Where $[K]$ is a square matrix of $L \times L$; the sub-matrix $[K_{i,j}]$ is a square matrix of order of $M + 2$, most of the elements of this matrix are 0, and its non-zero elements are

$$\left.\begin{aligned} K_{i,j}(l, l-1) &= -\alpha C_{ij,l} \\ K_{i,j}(l, l) &= \begin{cases} 2\alpha C_{ij,l} + 1, i = j \\ 2\alpha C_{ij,l}, i \neq j \end{cases} \quad l = 2, \cdots, M \\ K_{i,j}(l, l+1) &= -\alpha C_{ij,l} \end{aligned}\right\} \tag{31}$$

The constraint condition of equal displacement of pile top is required:

$$K_{i,j}(1,2) = \begin{cases} 1, j = i \\ -1, j = i+1 \end{cases} \tag{32}$$

The condition that the sum of axial forces of each pile is equal to the total load is as follows:

$$\left.\begin{aligned} K_{n,j}(1,1) &= \beta \\ K_{n,j}(1,3) &= -\beta \end{aligned}\right\} \tag{33}$$

Boundary conditions of pile tip:

$$\left.\begin{aligned} K_{i,j}(M+2, M) &= C_{\mathrm{b}ij} \beta \\ K_{i,j}(M+2, M+1) &= \begin{cases} -1, i = j \\ 0, i \neq j \end{cases} \\ K_{i,j}(M+2, M+2) &= -C_{\mathrm{b}ij} \beta \end{aligned}\right\} \tag{34}$$

3.2 Governing equations and solutions under temperature load

Under the action of temperature load, the form of the equilibrium equation remains unchanged. It only needs to consider the influence of temperature and modify the submatrix and the load vector locally according to the boundary conditions.

For bearing caps with large stiffness, the bottom surface of bearing caps remains flat after each pile experiences different temperature loads. If the origin of coordinates is taken at the center of No.1 pile (see Fig.1), then according to the rigid body deformation assumption of the foundation:

$$\delta u_{i,1} = \delta u_{1,1} + \delta\theta_y x_i + \delta\theta_x y_i \tag{35}$$

where $\delta\theta_x$, $\delta\theta_y$ are the increments of the rotation angle of the cap around x and y coordinate axes, respectively. For the convenience of derivation and solution, one pile on the x axis and one on the y axis are respectively marked as No. 2 pile and No. 3 pile. After $\delta\theta_x$ and $\delta\theta_y$ are expressed by displacement of the pile top, we have

$$-\left(1-\frac{x_i}{x_2}-\frac{y_i}{y_3}\right)\delta u_{1,1}-\frac{x_i}{x_2}\delta u_{2,1}-\frac{y_i}{y_3}\delta u_{3,1}+\delta u_{i,1}=0 \tag{36}$$

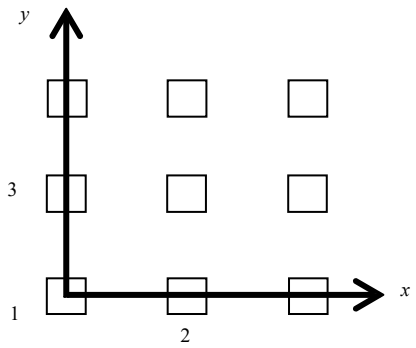

Fig. 1 Numbering rules for energy pile

According to Eq. (36), the first row of the sub-matrix $[K_{ij}]$ is cleared to zero, and is re-assigned as follows:

$$\left.\begin{aligned} K_{i,1}(1,2) &= -\left(1-\frac{x_i}{x_2}-\frac{y_i}{y_3}\right) \\ K_{i,2}(1,2) &= -\frac{x_i}{x_2} \\ K_{i,3}(1,2) &= -\frac{y_i}{y_3} \\ K_{i,i+3}(1,2) &= 1 \end{aligned}\right\} \quad i=1\sim n-3 \tag{37}$$

$$\left.\begin{aligned} &\sum_{i=1}^{n}\left(\beta\left(\delta u_{i,0}-\delta u_{i,2}\right)+\gamma\delta T_i\right)=0 \\ &\sum_{i=1}^{n}\left(\beta\left(\delta u_{i,0}-\delta u_{i,2}\right)+\gamma\delta T_i\right)x_i=0 \\ &\sum_{i=1}^{n}\left(\beta\left(\delta u_{i,0}-\delta u_{i,2}\right)+\gamma\delta T_i\right)y_i=0 \end{aligned}\right\} \tag{38}$$

where $\gamma = E_p A\alpha_T$, x_i and y_i are pile cap coordinates.

Equation (38) has only n−3 equations, and 3 additional equations are needed to solve it. Considering that the external load of the energy pile is constant, that is, the resultant force and resultant moment increments of each pile top reaction force are 0. According to Eq. (2), the axial force is expressed discretely:

The $(i = n-2)^{\text{th}}$ row of the matrix $[K_{ij}]$ represents the moment equilibrium condition around the y axis, there is

$$\left.\begin{aligned} K_{n-2,j}(1,1) &= \beta x_j \\ K_{n-2,j}(1,3) &= -\beta x_j \end{aligned}\right\} \quad j=1,\cdots,n \tag{39}$$

The $(i = n-1)^{\text{th}}$ row of the matrix $[K_{ij}]$ represents the moment equilibrium condition around the x axis:

$$\left.\begin{aligned} K_{n-1,j}(1,1) &= \beta y_j \\ K_{n-1,j}(1,3) &= -\beta y_j \end{aligned}\right\} \quad j=1,\cdots,n \tag{40}$$

The $(i = n)^{\text{th}}$ row represents conditions of force equilibrium:

$$\left.\begin{aligned} K_{nj}(1,1) &= \beta \\ K_{nj}(1,3) &= -\beta \end{aligned}\right\} \quad j=1,\cdots,n \tag{41}$$

Considering the influence of temperature, the boundary condition of pile tip becomes

$$\delta u_{i,M} = \sum_{j=1}^{n} C_{\mathrm{b}ij}\left[\beta\left(\delta u_{j,M-1}-\delta u_{j,M+1}\right)+\delta\Delta T_i\right] \tag{42}$$

The boundary conditions have no effect on the elements in $[K]$ matrix, temperature effects are incorporated in the load vector. Combined with the boundary condition of pile top, the load vector is zeroized and assigned as follows:

$$\left.\begin{aligned} F_{i,1} &= -\sum_{j=1}^{n}\gamma\Delta T_j x_j,\ i=n-2 \\ F_{i,1} &= -\sum_{j=1}^{n}\gamma\Delta T_j y_j,\ i=n-1 \\ F_{i,1} &= -\sum_{j=1}^{n}\gamma\Delta T_j,\ i=n \\ F_{i,M+2} &= -\sum_{j=1}^{n} C_{\mathrm{b}ij}\gamma\Delta T_j,\ i=1,\cdots,n \end{aligned}\right\} \tag{43}$$

Considering the nonlinear characteristics at the pile−soil interface, the governing equations were solved by the mid-point increment method. After the displacement of the pile, the axial force distribution and shear stress distribution, etc., could be obtained according to Eqs. (2) and (4).

3.3 Summary of parametric analysis

The main parameters used in this method include material elastic modulus E_p, pile diameter r, pile length l, pile spacing S, coefficient of thermal expansion α_T, pile temperature increment ΔT, soil shear modulus G, Poisson's ratio ν, pile side friction in limit equilibrium state τ_f, slip displacement in the limit equilibrium state s_f, ultimate pile tip resistance P_{bf}, failure stress ratio between pile side and pile end R_f. These parameters are in consistent with those from the traditional analysis method of pile foundation displacement under mechanical load and can be obtained conveniently.

4 Cases and validations

4.1 Case 1: Conventional pile group foundation under mechanical load

This case is taken from the field test results of 9 piles given by O'Neill et al.[22]. The pile is a closed steel pipe pile with a diameter of 273 mm and a wall thickness of 9.3 mm. The pile length is 13.1 m. The piles are arranged in a square with a center spacing of 819 mm. The foundation soil is a hard and over-consolidated clay. The shear modulus of the foundation soil increases linearly along the depth, which at the ground surface is 47.9 MPa, and at the pile tip is 151 MPa. The undrained shear strength of the soil is 47.9 kPa at the ground surface and 239 kPa at the end of the pile; the side friction resistance of the pile is taken as 0.34 c_u. The ultimate bearing capacity of the pile tip is estimated to be 9 c_u = 2.15 MPa. The above parameters are determined according to the suggestions of Chow et al.[23]. Under undrained loading conditions, the Poisson's ratio of the soil is assumed to be 0.5. Take 0.95 of R_f based on experience. The parameters a and b are determined according to Eqs. (7) and (8), and two cases of s_f = 2 and 4 mm are considered in the calculation. The parameters f and g are determined according to Eqs. (14) and (15).

The measured and calculated values of the load−settlement curves of pile group foundation is compared as shown in Fig. 2. In this case, the failure displacement of the contact surface has little effect on the calculation results. The calculated nonlinear relationship and magnitude of the load along with the settlement are in good agreement with the measured value, and the results of s_f = 4 mm are closer.

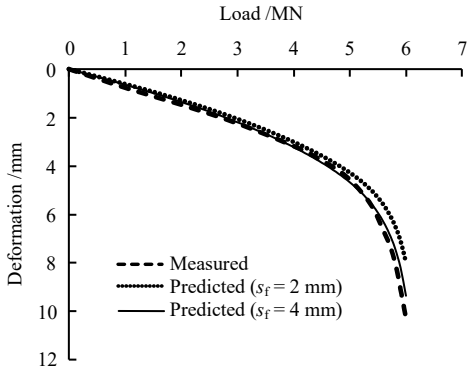

Fig. 2 Load−settlement curves of the pile group

Table 1 compares the load shared by each pile under the action of working load P_w = 2 580 kN. The specific positions of piles 1 to 3 are shown in Fig. 3. Similar to the actual measurement results, under the rigid raft connection condition, due to the interaction of the pile group, the corner piles bear the largest load, the side piles subject to intermediate load, and the center piles carry the smallest. Compared with the corner piles, the load on the center pile is about 7.4% (calculated value) and 9.2% (measured value) smaller.

Table 1 Load distribution on top of the pile group(Case 1)

Pile	Measured load /kN	Computed load /kN
Pile 1（Corner）	294	292.9
Pile 2（Side）	285	284.3
Pile 3（Center）	267	271.2

The distribution of side friction resistance of each pile under working load P_w and ultimate load P_u (5 670 kN) is plotted in Fig. 3. The results show that the side resistance of the upper part of the pile under working load is fully exerted and conforms to the general law. Since the corner piles bear relatively more loads, the side resistance is larger and the center pile bears the smallest resistance. When the load reaches the limit value, sufficient shear deformation has occurred on the pile−soil interface, the side resistance of each pile reaches the limit value, and the distribution tends to be consistent. Overall, the difference in shear stress at the pile−soil interface in the pile group foundation is not too large, and it is feasible to ignore the difference of each pile when analyzing the working characteristics of the pile group under mechanical load. In the foundation of energy pile group, however, the deformation and side resistance of the piles are not the same if only part of the piles are energy piles. At this time, the method proposed in this paper will have better adaptability.

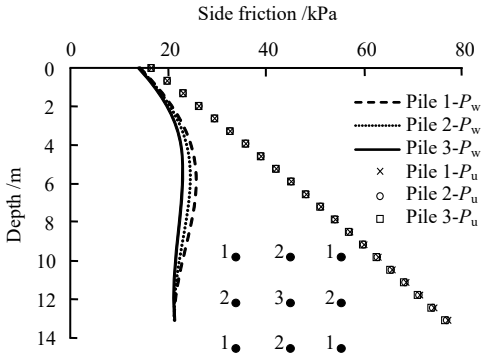

Fig. 3 Shear stress distribution on the shaft

4.2 Case 2: Energy pile group under integral variable temperature condition

Rotta et al.[16−17] studied the deformation characteristics of the energy pile group foundation under only the temperature load, and gave a design diagram of the interaction factor of the double energy pile system. This section uses the method proposed in this paper to do the prediction. In the calculation, two pile lengths, L = 25 m and L = 50 m, are considered. The diameter D = 1 m, the pile elastic modulus E = 30 GPa, the pile linear expansion coefficient is 10^{-5} ℃$^{-1}$, and the temperature increment is 10 ℃. The shear modulus of the soil is 30 MPa, and the Poisson's ratio is 0.3. The pile side friction resistance

is obtained empirically, which is 80 kPa, the ultimate resistance of the pile tip is 720 kPa, R_f is 0.9, and s_f is 4 mm. The parameters a, b, f and g are determined according to Eqs. (7), (8), (14), and (15), respectively.

The calculated results of the interaction factor Ω between this method and the Rotta's method[17] are compared as illustrated in Fig. 4. The definition of Ω is as follows: for 2 piles i and j, the uplift deformation at the top of pile j caused by elevating temperature of the pile is u_j, and the top deformation of the pile i in a single pile foundation under the same temperature increment is u_i, then $\Omega = u_j/u_i$. It can be seen from the figure that the calculated values of the two methods are in good agreement. When L/D = 25 and L/D = 50, the maximum values of Ω are around 0.13 and 0.30, respectively and they decrease with the normalized pile spacing S/D increases (S is the distance between the centers of the piles, and D is the diameter of the piles) until they stabilize. Note that the Rotta's method cannot consider the influence of the nonlinear shear characteristics of the pile−soil interface. If the side friction resistance is taken as 30 kPa, according to Eq.(7), the parameters on the pile−soil contact surface change accordingly, and the corresponding calculated results are shown by the dashed line in Fig. 4 (marked as this paper method-2), which indicates that after the strength of the pile−soil interface decreases, the mutual influence factor decreases. The larger the L/D, the lower the Ω.

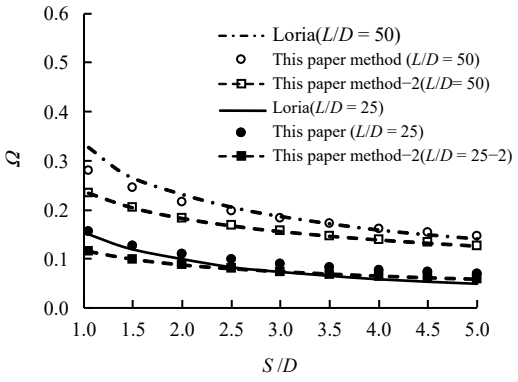

Fig. 4 Relationship between the interaction factor and the normalized pile spacing

After the interaction factor of two piles is obtained, the pile top deformation of each pile in pile group foundation can be calculated by the superposition principle. Because the interaction factor method does not consider the action of pile cap, it can only calculate the free condition. It is necessary to use the average deformation of all piles to represent the displacement of pile group. Figure 5 shows the normalized deformation u/D of a 5×5 pile group foundation. For comparison, the results of 3D finite element analysis are also presented. As shown in the figure, the displacement of pile group calculated by the interaction factor method is larger than that calculated by the finite element method. When the distance between pile centers is small, the error between the interaction factor method and the finite element method is obvious. This is because in pile group foundation, the deformation of pile body will decrease with the same temperature increment due to the influence of the stiffness of adjacent piles, which is not reflected in the interaction factor method.

Another characteristic of this method is that it can consider the constrained condition of pile top displacement and can be used in the case of pile top with rigid cap. Figure 6 compares the deformation distribution of 5 piles in diagonal with and without cap when S/D=3. When the pile top is free, the deformation of pile in the corner is the smallest, while pile in the center shows the largest deformation, with a difference of about 10%. When the piles are connected through the cap, the displacement of corner piles increases and that of the center piles decreases, which reflects the interaction between pile−cap−pile. Considering this effect is very important to analyze the working characteristics of energy pile group foundations.

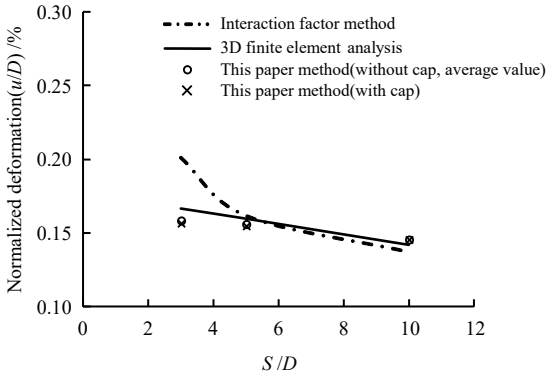

Fig. 5 Normalized displacement of a 5×5 energy pile group

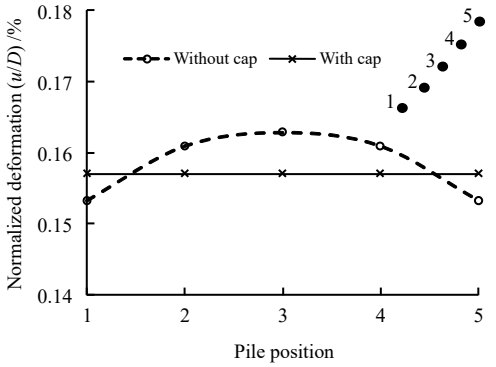

Fig. 6 Normalized pile displacement along the diagonal of a 5×5 energy group(S/D = 3)

4.3 Case 3: Energy pile group foundation with local piles subjected to temperature change

Ng et al.[12] conducted a centrifuge test on a 2×2 pile group foundation. The centrifugal acceleration is 60 g. Hollow steel pile is used in test, with a length of 550 mm, an external cross section of 20 mm×20 mm and a wall

thickness of 1.6 mm. The surface of the pile body is coated with 1.5 mm thick epoxy resin layer. The pile top is connected by 25 mm thick aluminum slab. The test first applied a mechanical load of 2.64 kN to the pile group foundation, and then cyclically changed the temperature of a pile with a temperature range of ±7 ℃ for a total of 10 cycles.

Numerical simulation was carried out under the prototype model, and the elastic modulus of sand was taken empirically as[24]

$$E = 60\,000 D_{\mathrm{r}} \sqrt{\sigma_3'/100} \tag{44}$$

where $\sigma_3' = K_0 \gamma' z$ is the effective small principal stress (kPa); γ' is the effective unit weight, taking 9.5 kN/m^3; K_0 is the horizontal earth pressure coefficient. The pile tip resistance is calculated by $N_{\mathrm{q}} \sigma_1'$, N_{q} is the bearing capacity coefficient. For soil with a friction angle of 31°, 20 may be taken for N_{q}. The pile side friction strength is calculated by σ_3' and δ, δ is the pile−soil interface friction angle, which is empirically taken as $0.8\varphi' = 25°$. The parameters a, b, f and g can be determined according to the method in section 2.2, $R_{\mathrm{f}} = 0.9$, $s_{\mathrm{f}} = 4$ mm. The elastic modulus of the steel pile is 206 GPa, and the thermal expansion coefficient is 1.5×10^{-5} ℃$^{-1}$.

For sand foundations, it is generally considered that there is a critical depth[25], and the side friction resistance and end resistance of the pile below the critical depth will no longer change. The critical depths in loose sand and dense sand are 15 and 20 times the side length B, respectively. In this case, 20 m is used, that is, the side friction resistance and end resistance of the pile at a depth below 20 m will no longer change.

Since the literature[12] does not give enough information, the horizontal earth pressure coefficient is determined by inversion of the ultimate bearing capacity. Figure 7 shows the simulation results of the load−settlement curve of a single pile under different values of K_0. When K_0 is set to 0.4, the ultimate bearing capacity determined according to the inflection point is closer to the 4 752 kN (prototype) given by Ng et al.[12], therefore, this paper takes $K_0 = 0.4$ in the subsequent analysis.

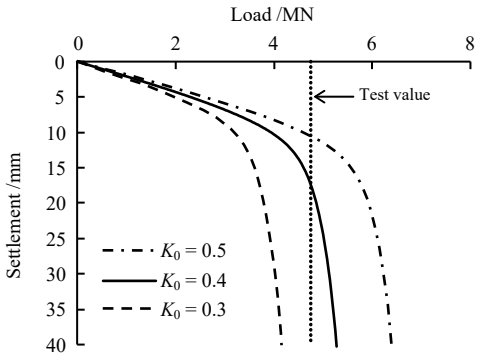

Fig. 7 Predicted load−settlement of the single pile

Figure 8 shows the change of the pile top displacement of each pile during the 10 cycles of temperature. The negative displacement in the figure represents the upward deformation. In the pile group foundation, only the pile 1 experienced temperature changes. During the first cycle of heating, the pile body was heated and expanded and the pile top was lifted by 1.5 mm. Under the rigid cap connection, the uplift of pile 1 causes the adjacent pile 2 and pile 3 to deform upward, but the pile 4 at the diagonal position shows downward displacement. The displacement directions of pile 1 and pile 4 are always opposite during the entire subsequent temperature change process, which means that the raft is deformed by rotation.

The foundation tilting obtained by Ng et al.[12] is shown in Fig. 9. The tilting in the figure is defined as the ratio of the settlement difference between the tops of pile 1 and pile 4 to the horizontal distance. A negative tilting means clockwise rotation around the line of piles 2 and 3. Since the simplified method in this paper does not consider the specific change process of temperature, only the range of temperature change is considered. Figure 9 only compares the calculated value with the actually measured value at the end of the temperature increase or decrease. Overall all, the calculated results of the tilting value are in good agreement with the measured results, and both increase gradually with the progress of the temperature cycles, and the increasing rate gradually decreases. The calculated and measured values of the maximum tilting are far less than 0.002 (shown by the dotted line in the figure), which is the tilting control standard of the towering structure foundation, and will not have much impact on normal use of pile ground.

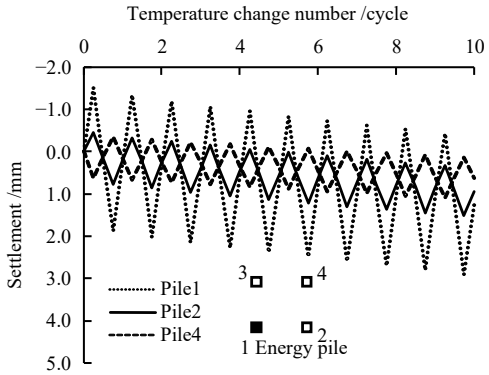

Fig. 8 Displacement at the pile head

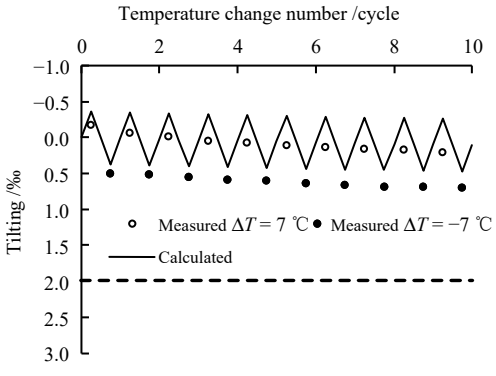

Fig. 9 Foundation tilting

The inconsistency of pile displacement will cause the redistribution of load on the pile top. The axial force distributions of each pile at the end of mechanical loading (before temperature rise) and after the first temperature rise are plotted in Fig. 10. The amount of axial force change caused by the temperature rise is also plotted in Fig. 10. For the four piles in square foundations, the distribution of the axial force of each pile along the pile length is the same after mechanical loading, showing the characteristics of typical friction piles. After the temperature rises, the pile 1 (energy pile) expands, and the top and tip of the pile deform upward and downward, respectively. Under the constraints of the other three ordinary piles, the upward displacement of the top of pile 1 is restricted, and the axial force on the top of the pile is increased by 505 kN (21% of the mechanical load). In addition, due to the restraint of the soil on the side of the pile, the friction of the soil at the upper part of the pile is reduced, and the friction of the soil at the lower part is increased. The position where the axial force of the No. 1 pile changes the most is about 15 m depth. The pile top displacement pattern is shown in Fig. 8, the pile top raft tilts after the temperature rises, the pile 4 is compressed downward, and the pile top load increases. Due to the requirement of moment balance, the axial force increment at the top of pile 4 will be consistent with pile 1. However, it should be pointed out that the change in axial force of pile 4 is mainly determined by the compression of the pile top. The change in axial force gradually decreases along the length of the pile, which is different from the convex distribution of axial force change in pile 1. In order to meet the balance condition, the load change values of pile 2 and pile 3 are opposite to that of pile 1. Based on the distribution of axial force change, we can conclude that the two piles are subjected to a pulling action, and the pile top load decreases during the heating process.

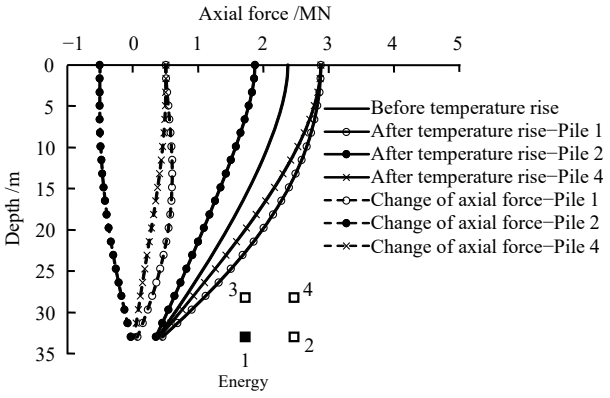

Fig. 10 Profiles of the axial force

Figure 11 shows the load variation on pile top with number of temperature cycles. Consistent with the actual measured value, the increase in temperature reduces the load on pile 2 while the decrease in temperature increases the load. As the temperature cycle progresses, the settlement of pile 1 gradually increases (see Fig. 8), making the load on pile 2 gradually increases. The maximum increase in temperature is about 33.8% during the temperature change, and an increase of 7% after completion of the temperature cycle.

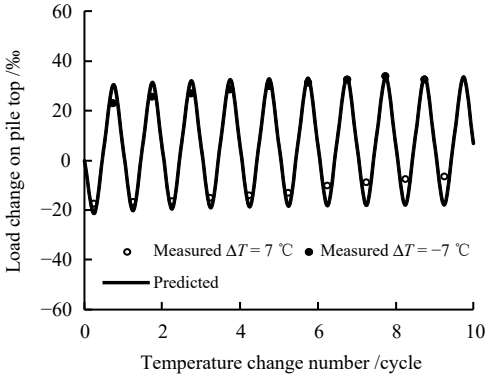

Fig. 11 Change of the applied load at the pile head

5 Conclusions

(1) In this paper, the hyperbolic model is used to reflect the relative slip displacement between pile and soil, the shear displacement method is used to model the transfer of shear stress in the soil, and the interaction between pile groups is considered. A simplified analysis method for the working characteristics of energy pile group foundation under coupled thermal−mechanical load is established.

(2) Compared with the interaction factor method, the proposed method can directly calculate the displacements and axial forces of all piles by considering the non-linearity of the pile−soil interface, the constraint conditions at the top of the pile and the position of the energy pile. Compared with the data in the literature, the proposed method can reasonably simulate the major working characteristics of energy pile group foundation, and has clear physical meaning and simple calculation features.

(3) The pile group effect of energy pile foundation is mainly due to the interaction of pile−soil and pile−raft. If only energy piles are presented locally, the pile-raft effect often plays a controlling role. With the development of differential deformation among piles, the foundation inclines and the pile top load redistributes. In the process of heating up, the load on the top of energy pile increases, while the load on the top of non-energy pile decreases.

(4) This method does not consider the influence of temperature change on the mechanical behaviors of soil and pile−soil interface. For cohesive soil whose mechanical properties change distinctly with temperature, the applicability of this method needs to be further studied.

References

[1] BRANDL H. Energy foundations and other thermo-active

ground structures[J]. Geotechnique, 2006, 56(2): 81−122.

[2] LIU Han-long, KONG Gang-qiang, NG C W W. Applications of energy piles and technical development of PCC energy piles[J]. Chinese Journal of Geotechnical Engineering, 2014, 36(1): 176−181.

[3] AMATYA B L, SOGA K, BOURNE-WEBB P J, et al. Thermo-mechanical behaviour of energy piles[J]. Géotechnique, 2012, 62(6): 503-519.

[4] GUI Shu-qiang, CHENG Xiao-hui. In-situ tests on structural responses of energy piles during heat exchanging process[J]. Chinese Journal of Geotechnical Engineering, 2014, 36(6): 1087−1094.

[5] LU Hong-wei, JIANG Gang, WANG Hao, et al. In situ tests and analysis of mechanical-thermo bearing characteristic of drilled friction geothermal energy pile[J]. Chinese Journal of Geotechnical Engineering, 2017, 39(2): 334−342.

[6] NG C W W, SHI C, GUNAWAN A, et al. Centrifuge modelling of heating effects on energy pile performance in saturated sand[J]. Canadian Geotechnical Journal, 2014, 52(8): 1045−1057.

[7] LALOUI L, NUTH M, VULLIET L. Experimental and numerical investigations of the behaviour of a heat exchanger pile[J]. International Journal for Numerical and Analytical Methods in Geomechanics, 2006, 30(8): 763−781.

[8] ROTTA LORIA A F, GUNAWAN A, SHI C, et al. Numerical modelling of energy piles in saturated sand subjected to thermo-mechanical loads[J]. Geomechanics for Energy and the Environment, 2015, 1: 1−15.

[9] FEI Kang, DAI Di, HONG Wei. A simplified method for working performance analysis of single energy piles[J]. Rock and Soil Mechanics, 2019, 40(1): 70−80.

[10] HUANG Yin-pei, JIANG Gang, LU Hong-wei, et al. Thermo-mechanical coupling load transfer method of energy pile based on exponential model[J]. Journal of Nanjing Tech University(Natural Science Edition), 2019, 41(1): 96−103.

[11] PENG H, KONG G, LIU H, et al. Thermo-mechanical behaviour of floating energy pile groups in sand[J]. Journal of Zhejiang University-Science A, 2018, 19(8): 638−649.

[12] NG C W W, MA Q J. Energy pile group subjected to non-symmetrical cyclic thermal loading in centrifuge[J]. Géotechnique Letters, 2019, 9(3): 173−177.

[13] LU Chen-kai, KONG Gang-qiang, SUN Guang-chao, et al. Field tests on thermal-mechanical coupling characteristics of energy pile in pile-raft foundation[J]. Rock and Soil Mechanics, 2019, 40(9): 3569−3575.

[14] SALCIARINI D, RONCHI F, CATTONI E, et al. Thermomechanical effects induced by energy piles operation in a small piled raft[J]. International Journal of Geomechanics, 2015, 15(2): 04014042.

[15] ROTTA LORIA A F, LALOUI L. Thermally induced group effects among energy piles[J]. Géotechnique, 2017, 67(5): 374−393.

[16] ROTTA LORIA A F, LALOUI L. The interaction factor method for energy pile groups[J]. Computers and Geotechnics, 2016, 80: 121−137.

[17] ROTTA LORIA A F, VADROT A, LALOUI L. Analysis of the vertical displacement of energy pile groups[J]. Geomechanics for Energy and the Environment, 2018, 16: 1−14.

[18] LEE K M, XIAO Z R. A simplified nonlinear approach for pile group settlement analysis in multilayered soils[J]. Canadian Geotechnical Journal, 2001, 38(5): 1063−1080.

[19] RANDOLPH M F, WROTH C P. Analysis of deformation of vertically loaded piles[J]. Journal of the Geotechnical Engineering Division, ASCE, 1978, 104(12): 1465−1488.

[20] PYKE R M. Nonlinear soil models for irregular cyclic loadings[J]. Journal of Geotechnical and Geoenvironmental Engineering, 1979, 105(6): 715−725.

[21] RANDOLPH M F, WROTH C P. An analysis of the vertical deformation of pile groups[J]. Geotechnique, 1979, 29(4): 423−439.

[22] O'NEILL M W, HAWKINS R A, MAHAR L J. Load transfer mechanisms in piles and pile groups[J]. Journal of the Geotechnical Engineering Division, 1982, 108(12): 1605−1623.

[23] CHOW Y K. Analysis of vertically loaded pile groups[J]. International Journal for Numerical and Analytical Methods in Geomechanics, 1986, 10(1): 59−72.

[24] BRINKGREVE R B J. Selection of soil models and parameters for geotechnical engineering application[C]// Proceedings of the Sessions of the Geo-Frontiers 2005 Congress. Austin, Texas: ASCE, 2005: 69−98.

[25] RANDOLPH M F, DOLWIN R, BECK R. Design of driven piles in sand[J]. Geotechnique, 1994, 44(3): 427−448.